

# Temporal Vectorization for Stencils

Liang Yuan

SKL of Computer Architecture, ICT,  
CAS  
yuanliang@ict.ac.cn

Hang Cao

SKL of Computer Architecture, ICT,  
CAS

Yunquan Zhang

SKL of Computer Architecture, ICT,  
CAS  
zyq@ict.ac.cn

Kun Li

SKL of Computer Architecture, ICT,  
CAS

Pengqi Lu

SKL of Computer Architecture, ICT,  
CAS

Yue Yue

SKL of Computer Architecture, ICT,  
CAS

## Abstract

Stencil computations represent a very common class of nested loops in scientific and engineering applications. Exploiting vector units in modern CPUs is crucial to achieving peak performance. Previous vectorization approaches often consider the data space, in particular the innermost unit-strided loop. It leads to the well-known data alignment conflict problem that vector loads are overlapped due to the data sharing between continuous stencil computations. This paper proposes a novel temporal vectorization scheme for stencils. It vectorizes the stencil computation in the iteration space and assembles points with different time coordinates in one vector. The temporal vectorization leads to a small fixed number of vector reorganizations that is irrelevant to the vector length, stencil order, and dimension. Furthermore, it is also applicable to Gauss-Seidel stencils, whose vectorization is not well-studied. The effectiveness of the temporal vectorization is demonstrated by various Jacobi and Gauss-Seidel stencils.

**Keywords** Stencil Computation, Vectorization, Data Alignment Conflicts

## ACM Reference format:

Liang Yuan, Hang Cao, Yunquan Zhang, Kun Li, Pengqi Lu, and Yue Yue. 2020. Temporal Vectorization for Stencils. In *Proceedings of ACM Conference, Washington, DC, USA, July 2017 (Conference'17)*, 12 pages.  
DOI: 10.1145/nnnnnnn.nnnnnnn

## 1 Introduction

The stencil computation is identified as one of the thirteen Berkeley motifs and represents a very common class of

nested loops in scientific and engineering applications, dynamic programming, and image processing algorithms. A stencil is a pre-defined pattern of neighbor points used for updating a given point. The stencil computation involves time-iterated updates on a regular  $d$ -dimensional grid, called the *data space* or *spatial space*. The data space is updated along the time dimension, generating a  $(d + 1)$ -dimensional space referred to as the *iteration space*. The stencils can be classified from various perspectives, such as the grid dimensions (1D, 2D, ...), orders (number of neighbors, 3-point, 5-point, ...), shapes (box, star, ...), dependence types (Gauss-Seidel, Jacobi) and boundary conditions (constant, periodic, ...).

The naive implementation for a  $d$ -dimensional stencil is comprised of  $(d + 1)$  loops where the outermost loop traverses the time dimension and the inner loops update all grid points in the  $d$ -dimensional spatial space. It exhibits poor data reuse and is a typical bandwidth-bound kernel. For improving the performance, blocking and vectorization are the two most powerful and commonly used transformation techniques.

There are two kinds of blocking methods for stencil computations: *spatial blocking* and *temporal blocking*. The spatial blocking algorithms promote data reuse in a single time step for 2D and higher dimension stencils by adjusting the data traversal pattern to an optimized order. An in-cache grid point may be reused to update all its neighbors before evicted from the cache. However, the locality exploited by space blocking is limited by the neighbor pattern size of a stencil. The temporal tiling [9, 22, 23, 26, 29, 38] takes the time dimension into consideration simultaneously with spatial dimensions. It has been exhaustively studied for stencils to further improve the data locality and alleviate the memory bandwidth demands.

The vectorization groups a set of data in a vector register and processes them in parallel to utilize vector units in modern CPU architectures. It exploits the data parallelism and serves to boost the in-core performance. There has been a long history of efforts to design efficient vectorization methods [1, 12, 16, 18, 21, 25, 31, 40]. Though the stencil computation is characterized by its apparently low arithmetic intensity, the vectorization is still profitable, especially for blocked stencil algorithms. Prior vectorization techniques for stencils focus on the data space, i.e. group points either in

---

Permission to make digital or hard copies of all or part of this work for personal or classroom use is granted without fee provided that copies are not made or distributed for profit or commercial advantage and that copies bear this notice and the full citation on the first page. Copyrights for components of this work owned by others than ACM must be honored. Abstracting with credit is permitted. To copy otherwise, or republish, to post on servers or to redistribute to lists, requires prior specific permission and/or a fee. Request permissions from [permissions@acm.org](mailto:permissions@acm.org).

*Conference'17, Washington, DC, USA*

© 2020 ACM. 978-x-xxxx-xxxx-x/YY/MM...\$15.00

DOI: 10.1145/nnnnnnn.nnnnnnn

the uni-stride space dimension [13] or multiple space dimensions [37]. We refer to this scheme as *spatial vectorization*.

One well-known problem induced by the spatial vectorization of stencils is the data alignment conflict. It arises from the fact that continuous vectors require the same value appears at different positions of vectors. Thus it incurs either redundant loads or additional data organization operations. Existing solutions [6, 13] reduce these overheads but still limit the performance or hurt the data locality. We will provide a detailed analysis in Section 2.

Furthermore, vectorization and blocking are often regarded as two orthogonal methods. However, the vectorization and tiling actually interact with each other for stencil computations. The vectorization often requires higher bandwidth and favors loading data from the first-level cache. On the contrary, the tiling tries to minimize the data transfer at the memory-cache level and prefers the last-level cache. This performance gap motivates our work and will be discussed in Section 3.1.

In this paper, we propose a novel *temporal vectorization* scheme considering the entire iteration space. A vector in the temporal vectorization scheme groups points with different time coordinates. It seeks to alleviate the data alignment conflict and bridges the above-mentioned performance gap. We also design a set of optimizations to alleviate weaknesses introduced by the new scheme and adjust the data layout to explore its potential.

The temporal vectorization still requires data reorganization operations, but the overhead is fixed and smaller than previous methods. Furthermore, a vectorization scheme usually only affects the single-core performance. However, the proposed temporal vectorization method leads to better utilization of the memory bandwidth. And in particular, it loads the data at a slower speed. Thus it can expect less memory contention especially for multi-core executions. We implemented the temporal vectorization with temporal blocking schemes and shows that the speedup increases with the number of cores especially for high-dimensional stencils. Finally, the temporal vectorization scheme is also applicable to the Gauss-Seidel stencils. Gauss-Seidel stencils update a point using the newest values of neighbor points. It is illegal to vectorize any single loop of the naive implementation code. To the best of our knowledge, we are not aware of vectorization methods for Gauss-Seidel stencils.

This paper makes the following contributions:

- We clarify a key characterization of stencils: the vectorization of stencils is sensitive to cache bandwidth and the blocking often favors a cache level with large capacity. The data alignment conflicts induced by vectorization enlarges this gap and is still unsolved by existing methods.
- We propose a novel temporal vectorization scheme for stencils. It expands the target scope of vectorization from the spatial space to iteration space. The

---

#### Algorithm 1: 1D3P Jacobi Stencil, scalar code

---

```

1 for ( t = 0; t < T; t = t + 1 ) {
2   for ( x = 1; x <= NX; x = x + 1 ) {
3     axt+1 = Stencil(ax-1t, axt, ax+1t);
4   }
5 }
```

---

temporal vectorization incurs a smaller fixed number of data reorganization operations and leads to a better data transfer rate than previous methods. Therefore it is less sensitive to the cache bandwidth. Furthermore, it is also applicable to Gauss-Seidel stencils.

- The effectiveness of the temporal vectorization is demonstrated by various Jacobi and Gauss-Seidel stencils.

The remainder of this paper is organized as follows. Section 2 provides the background. The temporal vectorization is described in Section 3. We present the performance results in Section 4. Section 5 overviews related work and Section 6 concludes the paper.

## 2 Background

### 2.1 Data Alignment Conflict of Vectorization

We take the 1D3P stencil as an example to illustrate the fundamental problem of the stencil computations caused by vectorization. The pseudo-code is listed in Algorithm 1.  $a_x^t$  represents the value at the point  $(t, x)$  in the iteration space where  $x$  and  $t$  are the coordinates in the space and time dimension, respectively. In each iteration of the inner space loop, it loads  $a_{x+1}^t$ , reuses in-register data  $a_{x-1}^t$  and  $a_x^t$  referenced by the previous calculation and writes the result  $a_x^{t+1}$  to memory. Observing the CPU-memory data transfer, one iteration of the inner loop is exactly similar to a common array copy algorithm.

The vectorization groups a set of data in a vector register and processes them in parallel. The naive vectorization of the 1D3P stencil code computes contiguous elements in the output array  $a_x^{t+1}$ . Assume the vector register holds 4 elements (i.e. vector length  $vl = 4$ ), the vectorization code performs the calculation with vector operations and outputs  $(a_1^{t+1}, a_2^{t+1}, a_3^{t+1}, a_4^{t+1})$  using one vector register.

A well-known problem incurred by the vectorization of stencil codes is the input data alignment conflicts. For example, to compute  $(a_1^{t+1}, a_2^{t+1}, a_3^{t+1}, a_4^{t+1})$ , it requires three vectors:  $(a_0^t, a_1^t, a_2^t, a_3^t)$ ,  $(a_1^t, a_2^t, a_3^t, a_4^t)$  and  $(a_2^t, a_3^t, a_4^t, a_5^t)$ . The element  $a_2^t$  appears in all these vector registers but at different positions.

The fundamental reason for the data alignment conflict is the data sharing between continuous calculations, e.g.,  $a_x^1$  and  $a_{x+1}^1$  depend on same points  $a_x^0$  and  $a_{x+1}^0$ . We refer to this as the *read-read dependence*. Conventionally the read-read dependence is not a data hazard as other data dependencies

**Algorithm 2:** 1D3P Jacobi Stencil, multi-load code

---

```

1 for ( t = 0; t < T; t = t + 1 ) {
2   for ( x = 1; x <= NX - 3; x = x + 4 ) {
3     v0 = vload(ax-1t, axt, ax+1t, ax+2t);
4     v1 = vload(axt, ax+1t, ax+2t, ax+3t);
5     v2 = vload(ax+1t, ax+2t, ax+3t, ax+4t);
6     (axt+1, ax+1t+1, ax+2t+1, ax+3t+1) = Stencil(v0, v1, v2);
7   }
8 }

```

---

including read-after-write, write-after-read, and write-after-write dependencies. Furthermore, common read-read dependence is usually exploited to promote data locality. However, for vectorized stencil codes, the data alignment conflict arises from the fact that components in one output vector or at the different positions of some output vectors have intra-vector or inter-vector read-read dependencies. Then the required data must redundantly appear in many vectors.

## 2.2 Existing methods

We present three existing solutions to the data alignment problem and discuss their drawbacks.

*Multiple load vectorization.* The common vectorization employed by production compilers loads all the needed vectors from memory straightforwardly as shown in Algorithm 2. Due to the low operational intensity, the stencil computation is often regarded as a memory-starving application. Compared with the scalar code, this multiple load vectorization method further increases the data transfer volume. Moreover, in each iteration of this code, it has at least two unaligned memory references where the first data address is not at a 32-byte boundary. Since CPU implementations favor aligned data loads and stores, these unaligned memory references will degrade the performance considerably.

*Data reorganization vectorization.* Another solution [6, 41] is similar to the scalar code in terms of the CPU-memory data transfer. It loads each input element to vector register only once and assembles the required vectors via inter-register data permutations instructions. Compared with the multiple load method, this data permutations method reduces the memory bandwidth usage and takes the advantages of the rich set of data-reordering instructions supported by most SIMD architectures. However, the execution unit for data permutations inside the CPU may become the bottleneck.

A common disadvantage of these two approaches is that the number of redundant data loads or reorganization operations increases with the order of a stencil, the length of the CPU vector register and the dimensionality of the problem. For example, to compute the vector  $(a_1^1, a_2^1, a_3^1, a_4^1)$  of the 1D5P stencil, it needs to put  $a_3^0$  in four vectors at all different positions to update  $a_1^1, a_2^1, a_3^1$  and  $a_4^1$ . Thus the redundancy is proportional to the order of a stencil and at most  $vl - 1$ . For

the 2D9P stencil, the innermost loop incurs two redundant loads and the outer space loop incur another four.

*Dimension-Lifting Transpose (DLT).* One milestone approach to address the data alignment conflict is the DLT method [13]. It turns to put the points with read-read dependencies in the same position of different vectors. Specifically, the original one-dimensional array of length  $N$  is viewed as a matrix of size  $vl \times (N/vl)$ . It then performs a matrix transpose. Consider the DLT method for a one-dimensional array of 28 elements. The second  $vl = 4$  elements in the transformed layout are contiguous stored and loaded into one output vector  $(a_1^1, a_8^1, a_{15}^1, a_{22}^1)$ . All the three required input vectors:  $(a_0^0, a_7^0, a_{14}^0, a_{21}^0)$ ,  $(a_1^0, a_8^0, a_{15}^0, a_{22}^0)$  and  $(a_2^0, a_9^0, a_{16}^0, a_{23}^0)$  are free of data sharing and also stored contiguously in memory. DLT only needs to assemble input vectors for calculating output vectors at boundary.

DLT has the following disadvantages. First, DLT can be viewed as  $vl$  independent stencils if we ignore the boundary processing. Therefore when incorporated with blocking frameworks, the data reuse decreases  $vl$  times. The reason is that there is no data reuse among the  $vl$  independent stencils. Second, DLT suffers from the overhead of explicit transpose operations executed before and after the stencil computation. For 1D and 2D stencils in scientific applications, the number of time loops is often large enough to amortize the transpose overhead. But for 3D stencils and low-dimensional stencils in other applications like image processing, the time size is often too small to amortize the overhead. Third, it's hard to implement the DLT transpose in-place and it often chooses to use an additional array to store the transposed data. This increases the space complexity of the code. Finally, DLT fails to apply to Gauss-Seidel stencils.

## 3 Temporal Vectorization

### 3.1 Motivation

Our work is motivated by two observations on the data transfers between the CPU and cache, and between the cache and memory.

First, the vectorized codes often achieve higher performance than scalar codes. Furthermore, the data alignment conflict induced by vectorization requires either more data transfers or data reorganization operations. Consequently, the vectorization increases the bandwidth demands. As will be demonstrated in the Evaluation section, all sequential non-blocking stencil implementations with existing vectorization techniques achieve the highest performance when the problem sizes fit in the L1 cache and the performance decreases fast as the problem size increases. Since the L2 cache provides competitive bandwidth compared with the L1 cache, it implies that existing vectorization schemes are relatively cache-bandwidth-sensitive.

Second, L1 cache sizes in modern CPUs are often small. The typical size is around 32 KB. It holds up to 4000 elements

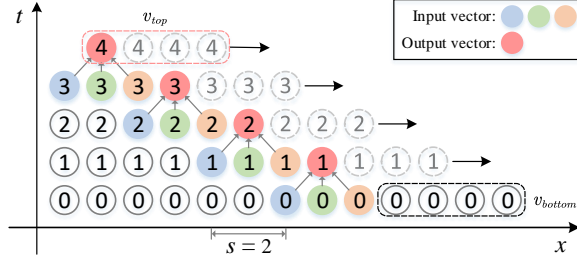


**Figure 1.** Temporal Vectorization of 1D3P Jacobi Stencil

for a double-precision floating-point kernel. Thus for higher dimension stencils the space blocking sizes and the corresponding temporal blocking size are limited, which will lead to a high memory transfer volume. As will be demonstrated in the Evaluation section, the parallel blocking stencil implementations with existing vectorization techniques often get the best performance when the block fits in L1 cache or L2 cache for one-dimensional or high-dimensional stencils. This demonstrates the memory-bandwidth-bound restriction should be first satisfied even it incurs a slower in-core performance for L2 cache. This indicates that the blocking scheme is cache-size-sensitive especially for high dimension stencils.

These two observations illustrate the trade-off between the data locality exploitation at cache-memory level and the in-core performance of the vectorized codes at the CPU-cache level. The conventional innermost loop vectorization leads to the best data reuse at the memory-cache level while incurs redundant CPU-cache data transfers.

The DLT generates an optimal in-core data access pattern while hurts the data locality in the cache. The sequential DLT results [13] exhibit performance improvements for all stencils when the data fit in caches. However, the DLT with a blocking scheme [14] derives considerable speedups for 1D stencils but only competitive or even worse performance for high-dimensional stencils. This implies that the degradation of data locality overweighs the benefits of the vectorization for the DLT.

We seek to design a vectorization scheme that maintains the data reuse ability and incurs a lightweight in-core data reorganizations simultaneously.

### 3.2 Algorithm

The key idea is to extend the vectorization scope from the data space to iteration space. Specifically, data points with different time coordinates are assembled in one vector. We take the one-dimensional Jacobi of double-precision floating-point data as an example and assume one vector holds four elements. The general form of a vector encapsulating point values in an one-dimensional stencil is  $(a_{x_3}^t, a_{x_2}^t, a_{x_1}^t, a_{x_0}^t)$ . For the stencil kernels used in the temporal vectorization, we

always set  $t_{i+1} - t_i = 1$ . The *space stride*  $s = x_i - x_{i+1}$  is determined by the stencil. Note that if it becomes the common vectorization in the multi-load and data reorganization approaches when  $t_{i+1} = t_i$  and  $s = 1$ , and DLT when  $t_{i+1} = t_i$  and  $s = NX/4$ .

To perform the stencil computation with a vector it only requires the elements in the vector are free of dependence. This is equivalent to respect the dependence defined by a stencil. Let the dependence set of a stencil be  $D$ . Each dependence  $(dt, dx) \in D$  implies that there exists two points  $(t', x')$  and  $(t'', x'')$  with  $t'' - t' = dt$  and  $x'' - x' = dx$  in the iteration space that  $a_{x''}^{t''}$  depends on  $a_{x'}^{t'}$ . It is easy to show that the temporal vectorization is legal when  $s > \max\{dx/dt | (dt, dx) \in D, dx > 0\}$ . We only consider dependencies with  $dx > 0$  since the innermost loop traverses the space dimension in increasing order. Take the 1D3P Jacobi stencil as an example, the dependencies are  $(1, 0)$ ,  $(1, 1)$  and  $(1, -1)$ . Thus it is sufficient to make the temporal vectorization legal by setting  $s > 1$ .

Algorithm 3 shows the pseudo-code of the temporal vectorization of the 1D3P Jacobi stencil with the space stride  $s = 2$ . Lines 2-4 update a small set of grid points at time  $t + 1$ ,  $t + 2$  and  $t + 3$  since the temporal vectorization assembles some of these pre-computed values of different time and

**Algorithm 3:** 1D3P Jacobi Stencil, temporal vectorization code with  $s = 2$

```

1 for ( $t = 0; t < T; t = t + 4$ ) {
2   Compute( $a_1^{t+1}, \dots, a_{2+2s}^{t+1}$ );
3   Compute( $a_1^{t+2}, \dots, a_{2+s}^{t+2}$ );
4   Compute( $a_1^{t+3}, \dots, a_{2+3s}^{t+3}$ );
5    $v_0 = \text{vloadset}(a_0^{t+3}, a_s^{t+2}, a_{2s}^{t+1}, a_{3s}^t)$ ;
6    $v_1 = \text{vloadset}(a_1^{t+3}, a_{1+s}^{t+2}, a_{1+2s}^{t+1}, a_{1+3s}^t)$ ;
7    $v_2 = \text{vloadset}(a_2^{t+3}, a_{2+s}^{t+2}, a_{2+2s}^{t+1}, a_{2+3s}^t)$ ;
8   for ( $x = 1; x \leq NX + 1 - 4s; x = x + 1$ ) {
9      $v_3 = \text{Stencil}(v_0, v_1, v_2)$ ; //  $v_3 = (a_{x+3}^{t+4}, a_{x+3}^{t+3}, a_{x+2s}^{t+2}, a_{x+3s}^{t+1})$ 
10     $v_0 = v_1$ ;
11     $v_1 = v_2$ ;
12    store( $a_x^{t+4}$ ); // Line 12-14 may be in different orders
13     $v_3 = \text{vrotate}(v_3)$ ; //  $v_3 = (a_{x+3}^{t+3}, a_{x+2s}^{t+2}, a_{x+3s}^{t+1}, a_x^{t+4})$ 
14     $v_2 = \text{vblend}(v_3, a_{x+4s}^t)$ ; //  $v_2 = (a_{x+3s}^{t+3}, a_{x+2s}^{t+2}, a_{x+3s}^{t+1}, a_{x+4s}^t)$ 
15  }
16  store( $v_0$ ); //  $v_0 = (a_{NX-3s-1}^{t+3}, a_{NX-2s-1}^{t+2}, a_{NX-s-1}^{t+1}, a_{NX-1}^t)$ 
17  store( $v_1$ ); //  $v_1 = (a_{NX-3s+0}^{t+3}, a_{NX-2s+0}^{t+2}, a_{NX-s+0}^{t+1}, a_{NX+0}^t)$ 
18  store( $v_2$ ); //  $v_2 = (a_{NX-3s+1}^{t+3}, a_{NX-2s+1}^{t+2}, a_{NX-s+1}^{t+1}, a_{NX+1}^t)$ 
19  Compute( $a_{NX}^{t+1}$ );
20  Compute( $a_{NX-s}^{t+2}, \dots, a_{NX}^{t+2}$ );
21  Compute( $a_{NX-2s}^{t+3}, \dots, a_{NX}^{t+3}$ );
22  Compute( $a_{NX-3s}^{t+4}, \dots, a_{NX}^{t+4}$ );
23 }
```

space coordinates. Lines 5-7 collect vectors for the first vectorized stencil computation. These vectors are called *input vectors* since they are fed to the vectorized stencil computing. Note that the values in one input vector are not stored contiguously in memory. So it must use strided load operations (e.g, gather or `_mm256_set_pd` intrinsics in Intel AVX). Line 9 performs the calculations and generates an *output vector*.

The temporal vectorization only requires the data reorganization of the *output vector* ( $a_x^{t+4}, a_{x+s}^{t+3}, a_{x+2s}^{t+2}, a_{x+3s}^{t+1}$ ). Since the next iteration of the outer time loop only requires the values with time coordinate  $t + 4$ , the component  $a_x^{t+4}$  at the highest position of the output vector is the actual output value of the innermost loop and must be stored to memory (Line 12). The other components should be moved to their left (higher) positions (Line 13) and blended with a new input element  $a_{x+4s}^0$  (Line 14). The assembled *input vector* ( $a_{x+s}^3, a_{x+2s}^2, a_{x+3s}^1, a_{x+4s}^0$ ) is used in subsequent stencil computations. Note that this vector can be either preserved in a CPU vector register or output to the memory for further use. Finally, Lines 19-22 calculate the rest values that are not covered by the vectorization code. Figure 1 illustrates the Algorithm. Note that the points with a same color are assembled in one vector.

This algorithm iteratively sweeps a time tile of the height equivalent to the vector length 4 and forwards all grid points from time coordinate  $t$  to  $t + 4$  in one iteration of the inner loop at Line 8. All the points in the iteration space with time coordinate  $t + i$  ( $t = 4k, i = 0, 1, 2, 3$ ) always appears at the  $i$ -th position of one input vector. Thus in the rest of the paper we can ignore  $t$  and always use  $(a_x^3, a_{x+s}^2, a_{x+2s}^1, a_{x+3s}^0)$  represents an input vector and  $(a_x^4, a_{x+s}^3, a_{x+2s}^2, a_{x+3s}^1)$  an output vector.

The values at the highest position of the output vectors in every four continuous iterations of the innermost loop are assembled in one *top vector*  $v_{top} = (a_{x+3s}^4, a_{x+2s}^4, a_{x+s}^4, a_x^4)$  and written to memory with a vector-storing instruction as shown in Figure 1. This task needs 5 data reorganization instructions. The first two values  $a_x^4$  and  $a_{x+s}^4$  are copied to the two lower positions of  $v_{top}$  after rotating their corresponding output vectors. The last two output values  $a_{x+2s}^4$  and  $a_{x+3s}^4$  are copied to the two higher positions of  $v_{top}$  before rotating their corresponding output vectors.

Similarly, the *bottom vector*  $v_{bottom} = (a_{x+4s+3}^0, a_{x+4s+2}^0, a_{x+4s+1}^0, a_{x+4s}^0)$  containing four continuous values with time coordinate 0 is loaded from memory by a vector-loading instruction and blended with four output vectors calculated in four continuous iterations to generate four corresponding input vectors. This task also requires 5 data reorganization operations. The temporal vectorization also needs one data reorder instruction to rotate the output vector or input vector. Thus the number of data reorganization operations per output vector is  $1 + 10/4 = 3.5$ .

*High-dimensional Stencils.* The temporal vectorization for one-dimensional stencils in effect performs a strip-mining to the outermost time loop and turns it into two nested

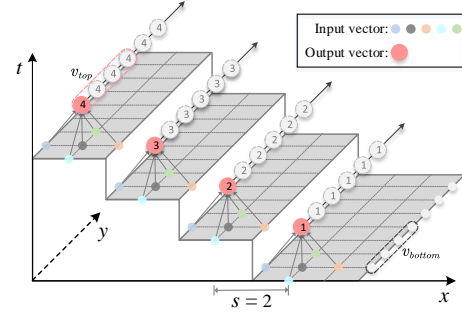


Figure 2. Temporal Vectorization of 2D5P Jacobi Stencil

time loops. The outer time loop index is incremented by the vector length while the inner time loop traverses a time tile. The temporal vectorization reorders the calculations in the inner time loop and the space loop. For high-dimensional stencils, it is illegal to interchange the inner time loop with space loops, thus it is only allowable to perform the temporal vectorization on the outermost space loop. Consequently, the pre-computation in Line 2-4 of Algorithm 3 forwards grid points in several lines for 2D stencils or planes for 3D stencils 1, 2, or 3 time steps. Figure 2 shows a pictorial view of the temporal vectorization of the 2D5P stencil.

The data transfer and vectorized computation in Line 5-18 of Algorithm 3 can be easily extended to higher dimensions. Note that there are additional space loops inside the  $x$  loop in Line 8. Therefore the reorganized input vectors, e.g.  $(a_{x+s,y}^3, a_{x+2s,y}^2, a_{x+3s,y}^1, a_{x+4s,y}^0)$  in a 2D stencil must be stored to memory for the next iteration of outer space loops, e.g. the computations in  $x + s - 1$ ,  $x + s$  and  $x + s + 1$  iterations.

### 3.3 Optimization

We now present several drawbacks introduced by the temporal vectorization and corresponding optimizations.

*Efficient data reorganization.* The first one is related to the data reorganization operations inside one iteration of the innermost loop in Algorithm 3. These operations must be executed sequentially. For example, to process the first output vector  $(a_x^4, a_{x+s}^3, a_{x+2s}^2, a_{x+3s}^1)$ , it needs permute it to  $(a_{x+s}^3, a_{x+2s}^2, a_{x+3s}^1, a_x^4)$ , copy out  $a_x^4$  and copy in  $a_{x+4s}^0$ . Note that the latter two operations have data dependence while the first reorganization can be arbitrarily permuted. Nevertheless, these three instructions have to be executed in order. Furthermore, in modern CPU architectures, the vector register is split to some 128-bit lanes. Data movements inside lanes incur a lower latency, typical 1 cycle versus 3 for lane-crossing instructions. The data reorganization instructions involving the bottom or top vectors are in-lane operations that incur small latency. Other instructions manipulating the output or input vectors solely, e.g., the rotation operation in Line 13 of Algorithm 3, are lane-crossing. Therefore these three instructions lead to a total latency of 5 cycles.



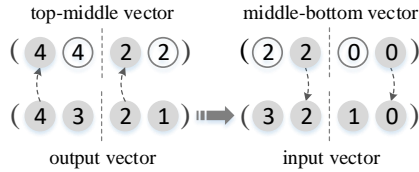


**Figure 3.** Reducing Lane-crossing Instructions

To reduce the latency, our key observation is that only  $a_{x+2s}^2$  in the output vector is moved across lanes for the corresponding input vector assembling. To reduce the latency of the data reorganization of one output vector and the number of lane-crossing instructions, we turn to copy out the value with the time coordinate 2 and copy in a new one which is already in the high lane.

To achieve this, we add another space stride (denoted as  $sl$ ) between lanes of the vector. Specifically, the form of output vectors becomes  $(a_x^4, a_{x+s}^3, a_{x+2s+sl}^2, a_{x+3s+sl}^1)$ . To form the corresponding input vector, both  $a_x^4$  and  $a_{x+2s+sl}^2$  are copied out to a *top-middle vector*. Then it is blended with a *middle-bottom vector* containing  $a_{x+2s}^2$  and  $a_{x+4s+sl}^0$  at different lanes to form the corresponding input vector  $(a_{x+s}^3, a_{x+2s}^2, a_{x+3s+sl}^1, a_{x+4s+sl}^0)$ . Thus the number of data reorganization instructions on the critical path is decreased to 2 and both of them can be implemented with in-lane instructions. Figure 3 illustrates this optimization. In this paper, we always set  $sl = 2$ .

To simplify the explanation of the top-middle and middle-bottom vector manipulations, the space coordinates are ignored. It is easy to extend it with  $x$  index and obtain the complete process. Every four iterations of the innermost loop generate two top-middle vectors of the form  $(a^4, a^4, a^2, a^2)$ . They can be combined with a bottom vector  $(a^0, a^0, a^0, a^0)$  to produce two middle-bottom vectors of the form  $(a^2, a^2, a^0, a^0)$  for subsequent input vector assembling. Finally, the two top-middle vectors are merged into a top vector. It needs 3 lane-crossing instructions to reorganize the top-middle and middle-bottom vectors, and the input and output vectors are no longer needed to be reorganized by lane-crossing instructions. In sum, the total number of data reorganization instructions is reduced to 3/4 lane-crossing and 2 in-lane instructions per vectorized stencil computation.

*Improving data parallelism for one-dimensional stencils.* The temporal vectorization also introduces dependence between input and output vectors in different iterations of the innermost loop. The reason is that there is data dependence along the time dimension and our vectorization scheme incorporates that dependence in iterations of the innermost space loop. For example, after calculating the output vector  $(a_1^4, a_3^3, a_5^2, a_7^1)$  of the current iteration  $x = 1$ , the calculation of  $a_2^4$  in the output vector  $(a_2^4, a_4^3, a_6^2, a_8^1)$  of the next iteration  $x = 2$  depends on  $a_3^3$ . This dependence resembles the common true (read-after-write) dependence. It limits the number

of concurrent instructions and may extremely impact performance.

One straightforward approach to increase the number of concurrent computations for the temporal vectorization of one-dimensional stencils is to widen the space stride  $s$ . As Figure 1 shows, the number of input vectors for one-dimensional Jacobi stencils is  $s + r$  where  $r$  is half of the stencil order. To determine the space stride  $s$ , one consideration is about the data reorganization process. Since a top vector groups the value of time coordinate 4 in every four output vectors, the number of available input vectors should be dividable by 4 to simplify the algorithm implementation. Another limitation to the upper bound of  $s$  is the number of available vector registers in the CPU. We conducted the experiments on CPUs with the AVX extension where the size of the vector register file is 16. Take the top, bottom, top-middle, middle-bottom and coefficients vectors into consideration, we always set the number of available input vectors to 8. Thus for the 1D3P Jacobi stencil, we set  $s = 7$ .

*Transposed data layout for high-dimensional stencils.* The temporal vectorization of one-dimensional stencils is able to keep the input vectors in CPU vector registers. Consequentially there is no memory transfer for the values with time coordinates 1, 2 and 3 computed in the inner loop. However, as explained above, since the temporal vectorization targets the outermost space loop of a high-dimensional stencil, the input vectors must be stored to memory for subsequent stencil computations. It is desirable to store the input vector contiguously.

Although the values in one input vector are not adjacent in the data space, the values with the same time coordinate at the same position of these input vector are stored contiguously in memory. For example, for four continuous input vectors  $(a_{x+s,y+i}^3, a_{x+2s,y+i}^2, a_{x+3s,y+i}^1, a_{x+4s,y+i}^0)$ , the four values with time coordinate 3,  $a_{x+s,y+i}^3$  ( $i = 0, 1, 2, 3$ ) logically occupy continuous positions. These four input vectors can be contiguously store in these spaces and actually can be viewed as a transposed layout.

*Initial input vectors loading (final output vectors storing).* The previous optimization improves the storage of the computed input vectors for high-dimensional stencils. The initial input vectors loading (Line 2-4 in Algorithm 3) and final input vectors storing (Line 16-18) can be implemented in a similar approach. These values are loaded to vectors by basic vector read instructions (e.g. `_mm256_load_pd`). Each vector contains values with a same time coordinate. Every four input vectors can be obtained by transposing corresponding vectors. Similarly, the final input vector is stored in memory after a transpose.

### 3.4 Implementation

We now present implementations of various stencils evaluated in this paper. The combination of the temporal vectorization and time-space blocks employed in parallelizations are also described.

*Jacobi stencils.* We implemented 1D3P, 2D5P, and 3D7P Heat equation stencils and a 2D9P stencil with non-periodic boundary conditions. They serve as the most important and most commonly used kernels in the study of compiler optimization, blocking scheme design, and vectorization of stencils. Applying the temporal vectorization with the optimizations to these Jacobi stencils is straightforward. For the 1D3P stencil, we set  $s = 7$  and use 13 vector registers including 7 input vectors, one top-middle vector, one middle-bottom vector, one top vector, one bottom vector, and two vectors for constant coefficients. For the 2D5P, 2D9P and 3D7P stencil we set  $s = 2$ .

For the parallel implementation, we use the diamond tiling [5] for the 1D3P stencil. Extending the non-blocking implementation to the diamond tiling code is simple. Each time tile of height 4 of a diamond is a trapezoid or inverted trapezoid. It only needs to change the loop boundary conditions for the blocking code implementation. For high-dimensional stencils, we adopt a diamond and parallelogram [35] hybrid tiling. The diamond tiling always applies to the outermost space loop and co-works with the temporal vectorization. The parallelogram tiling is performed on the rest space dimensions. For the space dimensions with parallelogram tiling, the corresponding indices must be shifted in input and output vectors. For example, the general form of the input vector becomes  $(a_{x,y}^3, a_{x+s,y+1}^2, a_{x+2s,y+2}^1, a_{x+3s,y+3}^0)$ . It is still straightforward to apply the optimizations.

*Game of life (Life).* Conway's Game of Life is a 2D9P Jacobi stencil where the stencil computation depends on the values of 8 neighbors. We adopt a particular variant called B2S23 used in Pluto [5]. Although it is sufficient to use one bit to represent the value (false for dead or true for live) at each grid point, we use the integer type like other works to facilitate the summation of values of 8 neighbors. The implementation of temporal vectorization and parallelization is similar to 2D5P and 2D9P Jacobi stencils.

*Gauss-Seidel stencils.* Gauss-Seidel stencils use the newest neighbor values to update one point. Conventionally it only requires one array to store the latest values of all grid points as opposed to two arrays in Jacobi stencils. Another difference between Jacobi and Gauss-Seidel stencils is that the latter contains data dependencies in all time and space loops. Thus it is illegal to perform the conventional innermost vectorization. Nevertheless, the implementations of Gauss-Seidel stencils are similar to Jacobi stencils. For the neighbors whose newest values are used in the calculation, the temporal vectorization uses their corresponding output vectors. It also leads to the same data reorganization cost to Jacobi stencils. We omit the detailed explanation. It is also illegal

to employ the diamond tiling for Gauss-Seidel stencils. Thus we utilize parallelogram tiling for all space dimensions.

*Longest common subsequence (LCS).* LCS is a classic problem solved by the dynamic programming method. It can be viewed as an 1D Gauss-Seidel stencil where the value  $lcs[x][y]$  on the point  $(x, y)$  in the iteration space represents the length of the longest common subsequence of two sequences  $A[1 \dots x]$  and  $B[1 \dots y]$ .  $lcs[x][y]$  depends on  $lcs[x-1][y]$ ,  $lcs[x-1][y-1]$ ,  $lcs[x][y-1]$ ,  $A[x]$  and  $B[y]$ . Thus the space stride must satisfy  $s \geq 1$ . To reduce the storage size, we view the  $x$  loop as the time dimension and  $y$  loop as space. Consequently the sequence  $B$  can be regarded as a variable coefficient. LCS allows the rectangle tiling in the iteration space. The implementation allocates two arrays  $lcsA[x]$  and  $lcsB[y]$  to store the values on the wavefront, i.e. the top and right boundaries of a rectangle.

### 3.5 Discussion

Compared with the multi-load vectorization method, our temporal vectorization method incurs no redundant data transfer. For one-dimensional stencils each value  $a_x^t$  only appears in one input vector. Furthermore, it is easy to align all the top and bottom vector transfers. For high-dimensional stencils  $a_{x,y}^t$  may be loaded in several continuous iterations ( $y-1, y$  and  $y+1$  for the 2D5P stencil) of the next-to-innermost space loop, but it still requires fewer data transfers to the multi-load vectorization.

Compared with the data reorganization approach, the number of data reorganization operations in our method is fixed and irrelevant to the vector length, the stencil order, and dimensionality. With the double-stride optimization, the temporal vectorization incurs 0.75 lane-crossing and 2 in-lane instructions. The data reorganization vectorization needs 1 lane-crossing and 2 in-lane instructions for the 1D3P stencil and more for higher-order and dimension stencils.

Compared with the DLT method, the temporal vectorization gives rise to a better reuse of the data in cache. Though the temporal vectorization also incorporates data transpose operations, it only processes a small set of points and the overhead can be amortized by stencil calculations.

The temporal vectorization, data reorganization approach, and DLT methods achieve the same reuse pattern to the scalar code. For example, it only needs to load one input vector to compute an output vector for the 1D3P stencil. Thus the memory transfer volumes of their blocking implementations are also similar. However, the temporal vectorization leads to slower transfer speed. Specifically, the straightforward vectorization method touches all the input points in the data space in one time step while the temporal vectorization loads these data in four time steps. It can then expect less memory bandwidth contention, especially in multi-core executions.

Furthermore, for the two arrays in Jacobi stencils, the output data  $a_x^4$  and input data  $a_x^0$  actually share the same

array. The input vectors can be stored a fixed range of the other array. Thus it actually uses one array for non-blocking Jacobi implementations and only stores the data in two arrays at boundaries for blocking implementations. Therefore the memory transfer volume is reduced by a factor of 2 for Jacobi stencils.

The temporal vectorization would be represented with a set of loop transformations, i.e. the strip-mining of the time loop, the time skewing of the inner time loop and outermost space loop, the loop-peel and finally the outer-loop vectorization. However, there are some difficulties to implement it with general compiler techniques. First, the temporal vectorization needs auxiliary variables, e.g. the extra arrays in the static coefficient method or the  $lcsA[x]$  in LCS. These auxiliary data often needs manual efforts [30]. Second, it often requires a transposed data layout for efficient vector loads for high-dimensional stencils that complicate the compiler transformations. Third, for one-dimensional stencils the data with time coordinates 1, 2 and 3 are reused in CPU registers and not stored into memory. Conventionally compilers are conservative to store data to memory as performed by the original code. Finally, for high-dimensional stencils, it is illegal to interchange the time loop and spaces loops, this complicates the outer-loop vectorization since it must be applied to a loop that contains more than one inner loop.

Nevertheless, given the temporal vectorization algorithms, it is straightforward to implement a code generator. As a comparison, the DLT method can be viewed as a combination of the strip-mining of the innermost loop and the outer-loop vectorization of the two innermost loops. A domain-specific framework for temporal vectorization of stencil computations can be designed similarly.

The temporal vectorization also resembles the wavefront method [34] (loop skewing). The wavefront method utilizes the parallelogram block shape in temporal tiling. The temporal tiling aims at exploiting the data reuse in caches and reducing the memory transfer volume, while the temporal vectorization primarily serves to lessen the bandwidth pressure between the CPU and cache.

**Table 1.** Problem and Blocking Sizes

Benchmark	Problem Size	our blocking	auto blocking
Heat-1D	$16000000 \times 6000$	$16384 \times 128$	$2048 \times 128$
Heat-2D	$8000^2 \times 2000$	$256^2 \times 64$	$256^2 \times 64$
2D9P	$8000^2 \times 2000$	$256^2 \times 64$	$256^2 \times 64$
Heat-3D	$800^3 \times 200$	$32^3 \times 8$	$32^3 \times 8$
Life	$8000^2 \times 2000$	$256^2 \times 32$	$128^2 \times 32$
GS-1D	$16000000 \times 6000$	$2048 \times 64$	$2048 \times 64$
GS-2D	$8000^2 \times 2000$	$128^2 \times 32$	$128^2 \times 32$
GS-3D	$800^3 \times 200$	$32^3 \times 32$	$32^3 \times 32$
LCS	$200000 \times 200000$	$4096 \times 4096$	$4096 \times 4096$

## 4 Evaluation

### 4.1 Setup

Our experiments were conducted on a machine made of two Intel Xeon E5-2670 processors with 2.70 GHz clock speed. Each processor contains 12 physical cores and each core owns a 32KB private L1 cache, a 256KB private L2 cache, and a unified 30MB shared L3 cache. We compiled the program with the ICC compiler version 19.1.1, using the optimization flag '-O3 -xHost'.

For each stencil kernel, we implemented a sequential code without any blocking scheme and a parallel code with a specific blocking scheme described above. The results of sequential codes exhibit the sensitivity to cache bandwidth, and serve to determine the blocking sizes for the parallel experiments. The parallel codes were scaled from uni-core to all the 24 cores. The problem sizes for various benchmarks are listed in Table 1. We simply tested all blocking sizes that are the power of two and symmetric for all spatial dimensions and show the one producing the best performance in Table 1. However, we observed that the performance is very sensitive to the tile sizes, but this requires significant effort in auto-tuning and should be done separately.

We compared our scheme with ICC auto-vectorization. The scalar performance is also plotted. The performance is reported using Gstencils/s, i.e. the number of points updated per second.

### 4.2 Results

*Jacobi Stencils.* Figure 4 shows the performance results of Jacobi stencils. Left subfigures exhibit the sequential results and the right subfigures show the parallel performance.

The temporal vectorization of the Heat-1D stencil achieves significant performance improvement over the auto vectorization and scalar code for problem size larger than 512. However, the auto-vectorization performs better than the temporal vectorization for smaller problem sizes. The reason is the transpose overhead of initial and final input vectors assembling in the temporal vectorization and this overhead can be amortized for larger sizes. The auto-vectorization curve likes a staircase that contains sharp falls at sizes of cache levels. This kind of performance curve is ubiquitous. For stencil computations, this demonstrates that the auto-vectorization is more sensitive to the cache bandwidth than the scalar code. On the contrary, the temporal vectorization produces a flatter curve due to fewer CPU-cache data accesses. It indicates that the temporal vectorization is less sensitive to the cache bandwidth. For the parallel results, they all produce similar scalabilities with speedup around 20x for 24-core over uni-core. For all scales, the temporal vectorization is 3x and 1.6x faster than the scalar code and the auto-vectorization, respectively.

The Heat-2D and 3D stencils are star stencils. For continuous output vector calculations, there is no data sharing



over outer space loops. Thus the data alignment conflict only exists in the uni-stride space dimension and the auto-vectorization makes an optimal vector utilization for other space dimensions. The benefits of the temporal vectorization may be overweighted by its downsides. For sequential results, the temporal vectorization still incur flatter curves than the auto-vectorization. It obtains competitive and worse performance for sizes smaller than last-level cache compared with the auto-vectorization for Heat-2D and 3D stencil, respectively. The parallel results are consistent with sequential performance. The temporal vectorization exhibits better scalabilities with large parallelism than the auto-vectorization, especially for Heat-2D. This again implies the better bandwidth utilization of the temporal vectorization. As demonstrated by existing work, the 3D7P Jacobi stencil exhibits limited improvements on new parallelization [2] and vectorization schemes [14]. Our results of Heat-3D reveal a similar phenomenon.

The 2D9P and Life stencils are box stencils. The auto-vectorization leads to data alignment conflicts on all space dimensions. Therefore the temporal vectorization achieves visible and similar improvements for both stencils. The Life stencil performs more operations than the 2D9P stencil. Thus the auto-vectorization is less sensitive to cache bandwidth as shown in the sequential figure. Furthermore, the scalability of 2D9P stencil is similar to that of Heat-2D and they both have a decline in the 24-core execution for the auto-vectorization. The temporal vectorization produces better scalabilities for both stencils due to fewer data accesses.

*Gauss-Seidel Stencils.* Figure 5 exhibits the performance results of all Gauss-Seidel stencils. The temporal vectorization achieves significant performance improvements for all Gauss-Seidel stencils over the scalar codes. All sequential executions of the scalar codes without blocking achieve a similar absolute performance of around 0.4 Gstencils/s. This demonstrates that Gauss-Seidel stencils are limited by data dependencies.

For the 1D sequential execution, it obtains a super-linear speedup of up to 4.4. The reason is that the temporal vectorization leads to better utilization of the memory bandwidth. The curve is similar to that of the Head-1D Jacobi stencil. For smaller problem size the *scalar ratio*, i.e. the percentage of points processed with scalar arithmetic operations is larger. For example, with the space stride  $s = 7$ , there are 84 points in a time tile need to be calculated by the scalar codes (Lines 2-4 and 19-22 in Algorithm 3). This leads to a scalar ratio of 16% for problem size  $NX = 128$  and 1% for  $NX = 2048$ .

For the parallel execution, both scalar and vectorization codes achieve good scalabilities. Compared with the single-core execution, the 24-core results reach speedup of 19.6 for the scalar code and 20.7 for the vectorization code respectively. These results are comparable to those of Jacobi stencils and demonstrate that the parallelogram tiling provides competitive scalabilities. The temporal vectorization

delivers an average speedup of 3.5 and a maximal speedup of 3.9 over the scalar code.

The LCS stencil result is similar to that of the 1D Gauss-Seidel stencil. It processes integer values with integer SIMD instructions and has a theoretical maximal speedup of 8. The scalar code performs either  $\max(lcs[x-1][y], lcs[x][y-1])$  or  $lcs[x-1][y-1] + 1$  for calculating  $lcs[x][y]$  depending on the equality of  $A[x]$  and  $B[y]$ . However, the temporal vectorization needs to execute all these computations and obtains the correct vector by a blend instruction with a mask vector of equalities. Thus we would expect smaller speedups compared with the 1D Gauss-Seidel stencil. Nevertheless,

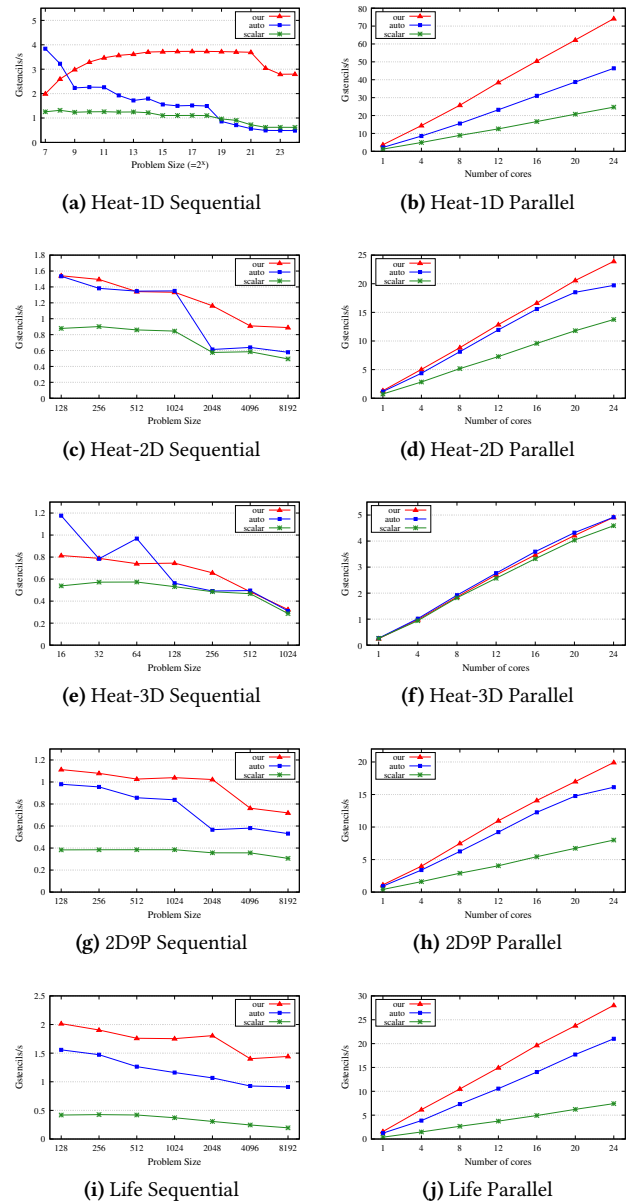


Figure 4. Jacobi Stencils

the temporal vectorization still achieves good improvements and yields an average speedup of 5.3 over the scalar code for the parallel execution.

For higher-dimensional Gauss-Seidel stencils, we see similar trends in sequential results but more sharp performance decreases when the problem size is larger than the L3 cache size. However, the in-cache performance is relatively steady and it demonstrates the less sensitivity to the cache bandwidth of the temporal vectorization. The maximal speedup is 3.8 for the 2D stencil with a problem size 2048<sup>2</sup> and 3.6 for the 3D stencil with a problem size 128<sup>3</sup>, respectively.

For the parallel experiments, both scalar and vectorization codes of the 2D and 3D stencil achieve good scalabilities, e.g. the speedup of 24-core over single core is 16.5 for scalar and 14 for vectorization. Compared with the scalar code, the temporal vectorization obtains an average speedup of 2.2 and 1.2 for 2D and 3D stencils, respectively.

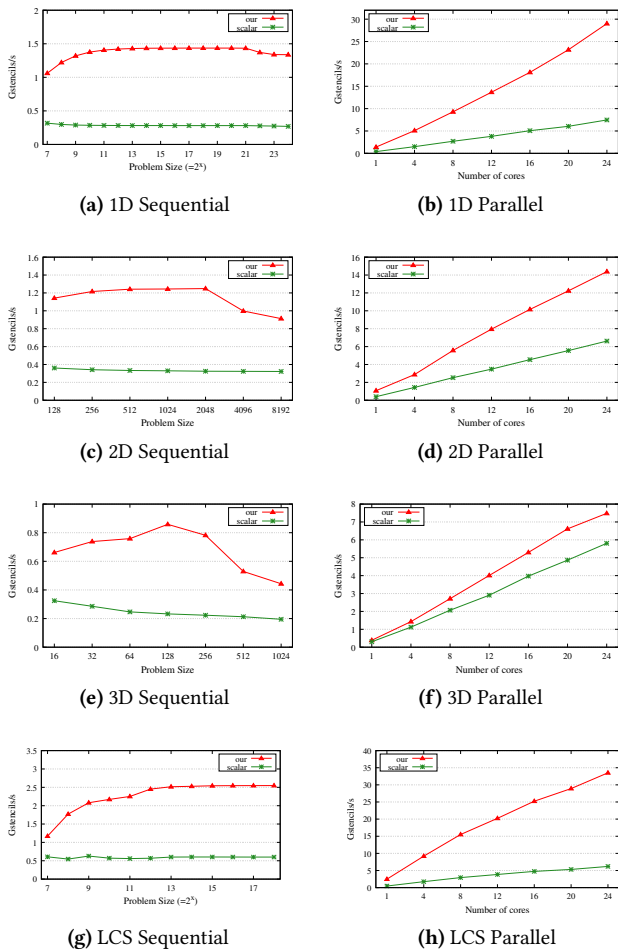


Figure 5. Gauss-Seidel Stencils

## 5 Related Work

The compiler community has been studying sophisticated universal vectorization techniques [1, 12, 16, 18, 25, 31]. Previous work [10, 19, 36] has proposed many solutions to address unaligned vector transfers. There are also many studies focusing on reducing the data preparation overhead [13, 28, 41]. The DLT [13] assembles points in the unit-stride space dimension that are free of intra-vector read-read dependencies in one vector. Other more general data organization Optimizations include data alignment optimization [4] and data interleaving [24, 41], However, some of these works are too general to capture the specific properties of stencils. For example, the data alignment conflicts for stencil refer to overlapped vector loads, it is unable to attack this problem by stream shifts [10].

The state-of-art compilers usually vectorize the innermost loop. Outer-loop vectorization techniques [25] often focus on the case where the innermost loop is illegal to be vectorized. One relaxed legality condition of the outer-loop vectorization is that it is interchangeable with the inner loop. However, the time loop is not interchangeable with space loops according to the data dependencies. Though more strict conditions exist, direct outer-loop vectorization at the time loop is still illegal. For slightly complicated codes, outer-loop vectorization requires auxiliary arrays and programmers need to explicitly declares them [30]. Some outer-loop vectorization techniques require the iteration number of the inner loop is invariant with respect to the outer-loop. However, many blocked stencil algorithms [11, 14, 33, 38] shrink or expand the data range in all space dimensions as the time proceeds. For example, the classic diamond tiling [17] introduces a diamond shape in the iteration space for a one-dimensional stencil. It enlarges the data space in the first half time and then decreases it in the rest time.

There exists a lot of work on improving the register reuse by utilizing the associative property of stencil calculations. The fundamental idea is to find a better order of statements across iterations. Deitz et al [8] proposes a compiler formulation and transformation called array common subexpression elimination. A similar idea called partial sum is also studied in [3]. Cruz and Araya-polo [7] and Stock et al [32] combine the gather (update an output element with all its neighbors) and scatter (update all its neighbors with one input element) patterns in one and many space dimensions, respectively. Several studies [15, 20, 27, 39] describe register reuse frameworks for GPUs. Yount [37] proposed a vector folding method to group points in the entire data space rather than a single dimension. However, prior work either targets scalar registers for high-order stencils on GPUs or specific stencils with constant and symmetrical coefficients. They only consider the reordering in one time step and data alignment conflicts are inevitable with vectorization. Furthermore, these methods are not applicable to and examined

for Gauss-Seidel stencils. The temporal vectorization preserves the same calculation order to the scalar code. Thus we believe this work can be incorporated into our scheme.

## 6 Conclusion

We have presented a new temporal vectorization scheme. It vectorizes the stencil computation in the whole iteration space and assembles points with different time coordinate in one vector. The temporal vectorization leads to a small fixed number of vector reorganizations that is irrelevant to the vector length, stencil order, and dimension. Furthermore, it is also applicable to Gauss-Seidel stencils. The effectiveness of the temporal vectorization is demonstrated by various Jacobi and Gauss-Seidel stencils. Future work will design a framework to automatically generate the stencil codes. We will also design an auto-tuning method to efficiently search the best block size.

## References

- [1] Randy Allen and Ken Kennedy. 1987. Automatic translation of Fortran programs to vector form. *ACM Transactions on Programming Languages and Systems (TOPLAS)* 9, 4 (1987), 491–542.
- [2] V. Bandishti, I. Pananilath, and U. Bondhugula. 2012. Tiling stencil computations to maximize parallelism (*SC '12*). 1–11.
- [3] Protonu Basu, Mary Hall, Samuel Williams, Brian Van Straalen, Leonid Oliker, and Phillip Colella. 2015. Compiler-Directed Transformation for Higher-Order Stencils (*IPDPS '15*). 313–323.
- [4] Aart J. C. Bik, Milind Girkar, Paul M. Grey, and Xinmin Tian. 2002. Automatic Intra-Register Vectorization for the Intel Architecture. *Int. J. Parallel Program.* 30, 2 (April 2002), 65–98.
- [5] Uday Bondhugula, Albert Hartono, J. Ramanujam, and P. Sadayappan. 2008. A Practical Automatic Polyhedral Parallelizer and Locality Optimizer (*PLDI '08*). 101–113.
- [6] Diego Caballero, Sara Royuela, Roger Ferrer, Alejandro Duran, and Xavier Martorell. 2015. Optimizing overlapped memory accesses in user-directed vectorization. In *Proceedings of the 29th ACM on International Conference on Supercomputing*. 393–404.
- [7] Raúl de la Cruz and Mauricio Araya-Polo. 2014. Algorithm 942: Semi-Stencil. *ACM Trans. Math. Softw.* 40, 3, Article 23 (April 2014), 39 pages.
- [8] Steven J. Deitz, Bradford L. Chamberlain, and Lawrence Snyder. 2001. Eliminating Redundancies in Sum-of-product Array Computations (*ICS '01*). 65–77.
- [9] Chris Ding and Yun He. 2001. A Ghost Cell Expansion Method for Reducing Communications in Solving PDE Problems (*SC '01*). 50–50.
- [10] Alexandre E Eichenberger, Peng Wu, and Kevin O'Brien. 2004. Vectorization for SIMD architectures with alignment constraints. *Acm Sigplan Notices* 39, 6 (2004), 82–93.
- [11] Matteo Frigo and Volker Strumpfen. 2005. Cache oblivious stencil computations (*ICS '05*). 361–366.
- [12] Mark Hampton and Krste Asanovic. 2008. Compiling for vector-thread architectures. In *Proceedings of the 6th annual IEEE/ACM international symposium on Code generation and optimization*. 205–215.
- [13] Tom Henretty, Kevin Stock, Louis-Noël Pouchet, Franz Franchetti, J. Ramanujam, and P. Sadayappan. 2011. Data Layout Transformation for Stencil Computations on Short-vector SIMD Architectures (*CC'11/ETAPS'11*). 225–245.
- [14] Tom Henretty, Richard Veras, Franz Franchetti, Louis-Noël Pouchet, J. Ramanujam, and P. Sadayappan. 2013. A Stencil Compiler for Short-vector SIMD Architectures (*ICS '13*). 13–24.
- [15] Mengyao Jin, Haohuan Fu, Zihong Lv, and Guangwen Yang. 2016. Libra: An Automated Code Generation and Tuning Framework for Register-limited Stencils on GPUs (*CF '16*). 92–99.
- [16] Ken Kennedy and John R. Allen. 2001. *Optimizing Compilers for Modern Architectures: A Dependence-Based Approach*. Morgan Kaufmann Publishers Inc., San Francisco, CA, USA.
- [17] Sriram Krishnamoorthy, Muthu Baskaran, Uday Bondhugula, J. Ramanujam, Atanas Rountev, and P. Sadayappan. 2007. Effective Automatic Parallelization of Stencil Computations (*PLDI '07*). 235–244.
- [18] Samuel Larsen and Saman Amarasinghe. 2000. Exploiting Superword Level Parallelism with Multimedia Instruction Sets. In *Proceedings of the ACM SIGPLAN 2000 Conference on Programming Language Design and Implementation (PLDI '00)*. Association for Computing Machinery, New York, NY, USA, 145–156.
- [19] Samuel Larsen, Emmett Witchel, and Saman Amarasinghe. 2002. Increasing and detecting memory address congruence. In *Proceedings. International Conference on Parallel Architectures and Compilation Techniques*. IEEE, 18–29.
- [20] Wen-Jing Ma, Kan Gao, and Guo-Ping Long. 2016. Highly Optimized Code Generation for Stencil Codes with Computation Reuse for GPUs. *Journal of Computer Science and Technology* 6, 31 (2016), 1262–1274.
- [21] Saeed Maleki, Yaoqing Gao, Maria J Garzar, Tommy Wong, David A Padua, and others. 2011. An evaluation of vectorizing compilers. In *2011 International Conference on Parallel Architectures and Compilation Techniques*. IEEE, 372–382.
- [22] Jiayuan Meng and Kevin Skadron. 2009. Performance modeling and automatic ghost zone optimization for iterative stencil loops on GPUs (*ICS '09*). 256–265.
- [23] A. Nguyen, N. Satish, J. Chhugani, C. Kim, and P. Dubey. 2010. 3.5-D Blocking Optimization for Stencil Computations on Modern CPUs and GPUs (*SC '10*). 1–13.
- [24] Dorit Nuzman, Ira Rosen, and Ayal Zaks. 2006. Auto-vectorization of interleaved data for SIMD. In *Proceedings of the 27th ACM SIGPLAN Conference on Programming Language Design and Implementation*. 132–143.
- [25] Dorit Nuzman and Ayal Zaks. 2008. Outer-loop vectorization: revisited for short SIMD architectures. In *Proceedings of the 17th international conference on Parallel architectures and compilation techniques*. 2–11.
- [26] Fabrice Rastello and Thierry Dauxois. 2002. Efficient Tiling for an ODE Discrete Integration Program: Redundant Tasks Instead of Trapezoidal Shaped-Tiles (*IPDPS '02*). 138–.
- [27] Prashant Singh Rawat, Fabrice Rastello, Aravind Sukumaran-Rajam, Louis-Noël Pouchet, Atanas Rountev, and P. Sadayappan. 2018. Register Optimizations for Stencils on GPUs (*PPoPP '18*). Association for Computing Machinery, New York, NY, USA, 168–182.
- [28] Gang Ren, Peng Wu, and David Padua. 2006. Optimizing data permutations for SIMD devices. In *Proceedings of the 27th ACM SIGPLAN Conference on Programming Language Design and Implementation*. 118–131.
- [29] Gabriel Rivera and Chau-Wen Tseng. 2000. Tiling Optimizations for 3D Scientific Computations (*SC '00*). Article 32.
- [30] Nadathur Satish, Changkyu Kim, Jatin Chhugani, Hideki Saito, Rakesh Krishnaiyer, Mikhail Smelyanskiy, Milind Girkar, and Pradeep Dubey. 2012. Can traditional programming bridge the Ninja performance gap for parallel computing applications?. In *ISCA*. 440–451.
- [31] Narasimhan Sreeraman and Ramaswamy Govindarajan. 2000. A vectorizing compiler for multimedia extensions. *International Journal of Parallel Programming* 28, 4 (2000), 363–400.
- [32] Kevin Stock, Martin Kong, Tobias Grosser, Louis-Noël Pouchet, Fabrice Rastello, Jagannathan Ramanujam, and Ponnuswamy Sadayappan. 2014. A framework for enhancing data reuse via associative reordering. In *PLDI*. 65–76.
- [33] Yuan Tang, Rezaul Alam Chowdhury, Bradley C. Kuszmaul, Chi-Keung Luk, and Charles E. Leiserson. 2011. The Pochoir Stencil Compiler (*SPAA '11*). 117–128.
- [34] Michael Wolfe. 1986. Loop skewing: the wavefront method revisited. *International Journal of Parallel Programming* 15, 4 (1986), 279–293.

- [35] David Wonnacott. 2002. Achieving Scalable Locality with Time Skewing. *Int. J. Parallel Program.* 30, 3 (June 2002), 181–221.
- [36] Peng Wu, Alexandre E. Eichenberger, and Amy Wang. 2005. Efficient SIMD Code Generation for Runtime Alignment and Length Conversion. In *Proceedings of the International Symposium on Code Generation and Optimization (CGO '05)*. IEEE Computer Society, USA, 153–164.
- [37] Charles Yount. 2015. Vector Folding: Improving Stencil Performance via Multi-Dimensional SIMD-Vector Representation (*HPCC-CSS-ICISS '15*). IEEE Computer Society, USA, 865–870.
- [38] Liang Yuan, Yunquan Zhang, Peng Guo, and Shan Huang. 2017. Tessellating stencils. In *Proceedings of the International Conference for High Performance Computing, Networking, Storage and Analysis*. 1–13.
- [39] Tuowen Zhao, Protonu Basu, Samuel Williams, Mary Hall, and Hans Johansen. 2019. Exploiting reuse and vectorization in blocked stencil computations on CPUs and GPUs. In *SC*. 1–44.
- [40] Hao Zhou and Jingling Xue. 2016. A compiler approach for exploiting partial SIMD parallelism. *ACM Transactions on Architecture and Code Optimization (TACO)* 13, 1 (2016), 1–26.
- [41] Hao Zhou and Jingling Xue. 2016. Exploiting mixed SIMD parallelism by reducing data reorganization overhead. In *CGO*. IEEE, 59–69.